Sensorless vector control for super-high speed PMSM drive

Bon-Ho Bae*, Seung-Ki Sul*, Jeong-Hyeck Kwon** and Jong-Sub Shin**
*School of Electrical Engineering & Computer Science, Seoul National University
San 56-1, Shillim-Dong, Kwanak-Ku, Seoul, Korea (ZIP 151-742)
Tel : +82-2-880-7243 Fax : +82-2-878-1452 E-mail : sulsk@plaza.snu.ac.kr
**Turbo Machinery Development, Engine Engineering Center, SAMSUNG TECHWIN Co., LTD.

Abstract- **This paper describes the implementation of the vector control schemes for a variable-speed 131kW PMSM (Permanent Magnet Synchronous Motor) in super-high speed application. The vector control with synchronous reference frame current regulator has been implemented with the challenging requirements such as the extremely low stator inductance(28μH), the high dc link voltage(600V) and the high excitation frequency(1.2kHz). Because the conventional position sensor is not reliable in super-high speed, a vector control scheme without any position sensor has been proposed. The proposed sensorless algorithm is implemented by processing the output voltage of the PI current regulator, and hence the structure is simple and the estimated speed is robust to the measurement noise. The experimental system has been built and the proposed control has been implemented and evaluated. The test result, up to the speed of 60,000 r/min, shows the validity of the proposed control.**

I. INTRODUCTION

The super-high speed drives are becoming attractive in many applications such as micro-turbine generators, centrifugal compressors and pumps. By the super-high speed operation, the system can be much smaller and lighter for the same power level. In the case of the mirco-turbine generator of 50kW, the weight can be one fourth of the diesel generator [1].

In the industrial field, the development of the high-speed centrifugal air compressor is a hot issue and many companies are involved [2]. Compared with the conventional air compressor of the positive displacement type, the high speed centrifugal compressors have many merits such as the simple structure, light weight, small size, high efficiency and so on. But it requires very high rotating speed. Some comparative studies are carried out for the various motors for this application [2~4]. In this paper, mainly because of the efficiency, the PMSM (Permanent Magnet Synchronous Motor) is used.

Because of the high efficiency, the PMSM fed from the inverter has been put into practice in a wide variety of the speed control applications. But the super-high speed PMSM has been put into practice recently by the development in the permanent magnet, binding materials, motor design method and bearing technology.

In this paper, the super-speed operation of 131kW PMSM is discussed. The cost effective and optimized power circuits are proposed. The synchronous reference frame current regulator for the small stator inductance and high dc link voltage is implemented and the operation of current regulator has been tested up to the excitation frequency of 1,200 Hz. And the vector control scheme without the speed/position sensors is proposed. In the proposed sensorless algorithm, the speed is estimated by processing the output voltage of the PI current regulator. The structure is simple and the estimated speed is robust to the measurement noise. The experimental system has been built and the proposed controls have been implemented and evaluated with and without the discrete hall sensors. The test results, up to the speed of 60,000 r/min, are presented.

II. SYSTEM OVERVIEW

Fig.1 shows the power circuit diagram of the developed super-high speed PMSM drive and the parameters of the PMSM are described in Table. I. In many conventional approaches, for the easy of current regulation, a buck or boost converter has been used to vary the dc link voltage. But in the proposed system, the constant dc link(600V) through the simple diode rectifier is adopted for the cost-effectiveness and the reliability of the system. A DC link inductor is used to improve the power factor of the utility. And three 1,200V, 300A IGBT's are connected parallel to compose a switch for the inverter. A regenerative resistor is provided to prevent the over-voltage, which can be caused by the rapid deceleration of the motor. To achieve the sinusoidal current control up to the excitation frequency of 1,200 Hz, the switching frequency of the inverter is set to 15 kHz. The high switching frequency increases the thermal dissipation of the devices and the thermal control is an important design issue. In the proposed system, the water-cooling is adopted for the thermal control of the stator of PMSM and the inverter. By using the water-cooling, the physical size of the heat sink is remarkably shrunk compared with that of air-cooling system. The asymmetric SVPWM (Space Vector PWM) is applied and the control period is set to 33.33 μs. Because the general-purpose microprocessors cannot meet the required calculation time, the TMS320VC33-150 DSP based digital controller is developed for the implementation. The experimental data have shown that it takes less than 20 μs to perform the vector control scheme including the proposed sensorless algorithm. To monitor the angle of the rotor, three discrete hall-effect sensors with a sensing magnet are installed in the motor. These signals can provide the mechanical angle information with the resolution of 60°.

TABLE I.
PARAMETERS OF PMSM

Number of Poles	2
Rated output [kW]	131
Rated speed [r/min]	70,000
Rated voltage [V_{rms}]	360
Rated torque [Nm]	17.9
Rated current [A_{rms}]	237
Stator resistor, Rs [Ω]	0.0055
Stator inductance, Ls [μH]	28

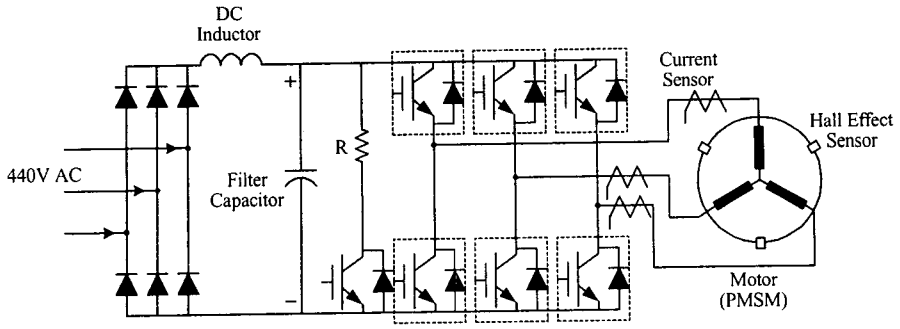

Fig. 1. Power circuit diagram of the proposed super-high speed PMSM drive.

For the operation up to super-high speed, the PMSM has been installed with special bearings. Because of the operational characteristics of the bearing, it is required to accelerate rapidly over the threshold speed range (about 6,000~9,000 r/min) in order to reduce the mechanical wear.

III. Design And Evaluation Of Current Regulator

The synchronous reference frame current regulator has become the industry standard for the current regulation of polyphase ac machines due to its capability of regulation of ac signals over a wide frequency range[5,6]. In the proposed system, the design of the synchronous reference frame current regulator has been a challenging job because of the high dc link voltage, the extremely small inductance and the high power rating. In order to evaluate the feasibility of the synchronous reference frame current regulator, the proceeding experiments have been carried out with the three-phase inductor load, which has the same inductance as the stator of PMSM.

Because of the high power rating and high dc link voltage, the dead-time is set to 3 μs and this is relatively large considering the short PWM period, 33.33 μs. So the precise compensation of the dead-time effect is a critical issue. For the effective voltage synthesis with SVPWM, the techniques in [7,8] are implemented. Because the ripple current is inevitably large, the precise current sampling is another important issue. The analog circuit has been designed to avoid delay, noise and the calibration for the current sampling is applied [10]. Fig. 2 shows the block diagram of the synchronous reference frame current regulator with the inductor load. The transformation, $T(\theta_e)$, is given by

$$T(\theta_e)=\frac{2}{3}\begin{bmatrix}\cos\theta_e & \cos(\theta_e-\frac{2}{3}\pi) & \cos(\theta_e+\frac{2}{3}\pi)\\ -\sin\theta_e & -\sin(\theta_e-\frac{2}{3}\pi) & -\sin(\theta_e+\frac{2}{3}\pi)\\ \frac{1}{\sqrt{2}} & \frac{1}{\sqrt{2}} & \frac{1}{\sqrt{2}}\end{bmatrix} \quad (1)$$

where the angle, θ_e, is the angle between the synchronous reference frame and the stationary frame.

Fig. 3 presents the experimental results with the proposed current regulator. For the test, a 3-phase air-core reactor is used and the inductance is set to the stator inductance of the PMSM, 28 μH.

From top to bottom, the graphs show three phase currents sampled by the controller, i_{as}, i_{bs}, i_{cs} and the c-phase current measured by the current probe set (Tektronix CT-4, A6302 and AM503), $i_{cs\text{-}m}$. The graphs of Fig. 3(a) present the experimental results with the excitation frequency of 20 Hz. From the results of (a), it is found that the performance of the current regulator is degraded at the zero crossings of the phase currents because of the effect of the dead-time and zero-current clamping even after careful compensation [7,8,10]. The graphs of Fig. 3(b) show the experimental results with the excitation frequency of 1,200 Hz. Because the dead-time effect and zero-current clamping effect are mitigated at high frequency, the currents are well controlled sinusoidaly without the degradation. But the measured current, $i_{cs\text{-}m}$, in (a), (b) of Fig. 3 presents large ripples due to the very small load inductance. The delay of the sampled current, i_{cs}, to the measured current, $i_{cs\text{-}m}$, is caused by the

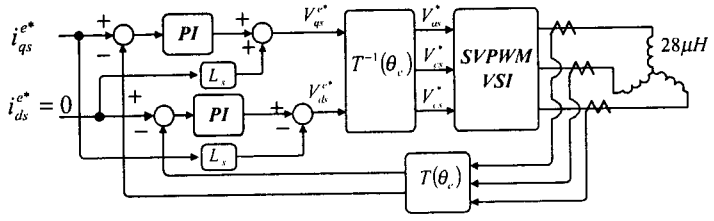

Fig. 2. Block diagram of synchronous reference frame current regulator with inductor.

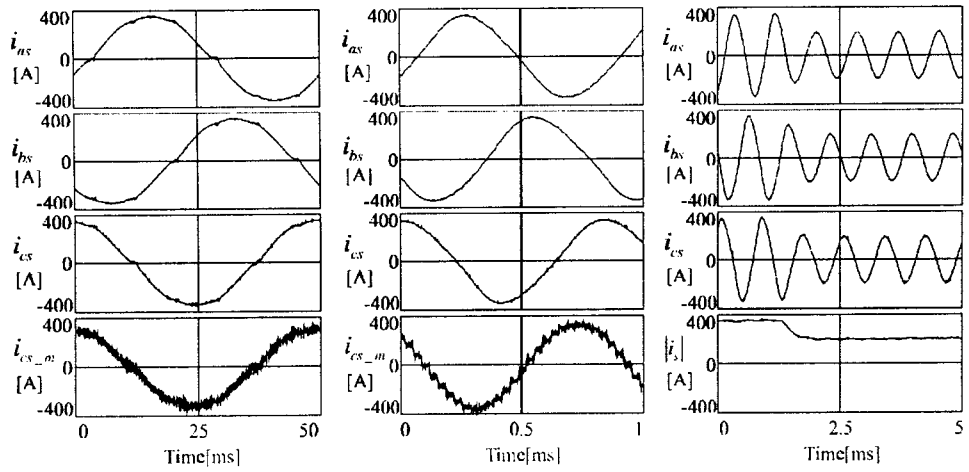

(a) (b) (c)

Fig. 3. Current waveform of synchronous reference frame current regulator with an inductor load.
(a) Current waveform with excitation frequency of 20 Hz.
(b) Current waveform with excitation frequency of 1200 Hz.
(c) Current waveform with excitation frequency of 1200 Hz .
(Magnitude of current reference is changed from 350 A_{peak} to 200 A_{peak}).

dealy of the serial D/A converter from which i_{cs} comes and low pass filter circuit. The graphs of (c) show the dynamic charactistic of the current regulator at the frequency of 1,200 Hz, The magnitude of the current reference is changed from 350 A_{peak} to 200 A_{peak}. The bottom graph of (c) is the magnitude of current vector, $|i_s|$. The three phase currents are well regulated sinusoidaly in a wide frequency range by the synchronous current requlator and the response is fast enough for the application

IV. Sensorless Vector Control Scheme without Any Position Sensor

Fig. 4 presents the block diagram of the sensorless vector control scheme without the position sensor. In the block diagram, the feed-forward terms, $V^e_{ds\_ff}, V^e_{qs\_ff}$, for the decoupling control are given by

$$V^e_{ds\_ff} = R_s i^{e*}_{ds} - L_s \hat{\omega}_r i^{e*}_{qs} \tag{2}$$

$$V^e_{qs\_ff} = R_s i^{e*}_{qs} + L_s \hat{\omega}_r i^{e*}_{ds} + \hat{\omega}_r \lambda_f . \tag{3}$$

where the $\hat{\omega}_r$ is the estimated speed of rotor.

Neglecting electrical transient, the voltage equations of the PMSM in the estimated reference frame can be presented by

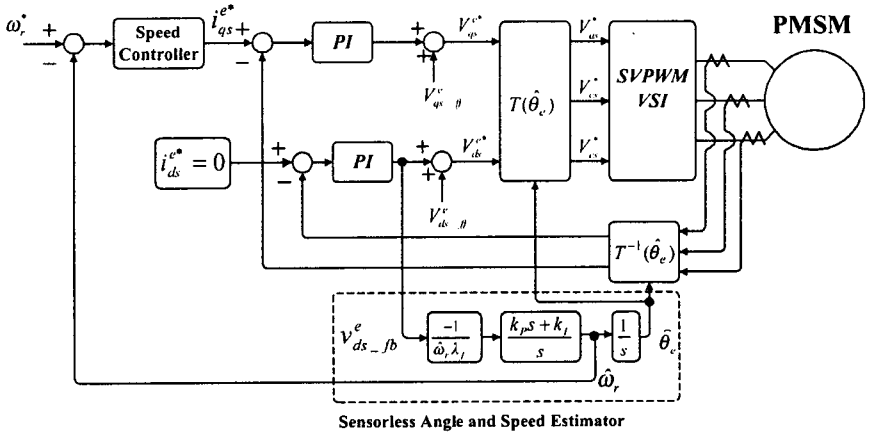

Fig. 4. Block diagram of sensorless vector control scheme without position sensor.

$$v_{ds}^{e} = R_s i_{ds}^{e} - \omega_r L_s i_{qs}^{e} + \omega_r \lambda_f \sin\theta_{err} \quad (4)$$

$$v_{qs}^{e} = R_s i_{qs}^{e} + \omega_r L_s i_{ds}^{e} + \omega_r \lambda_f \cos\theta_{err} . \quad (5)$$

where the angle error, θ_{err}, is the error between the real angle of the rotor, θ_r, and the estimated angle, $\hat{\theta}_e$.

$$\theta_{err} = \hat{\theta}_e - \theta_r . \quad (6)$$

From the relation of (2) and (4), the d-axis voltage error which has to be compensated by the d-axis PI(proportional and integral) regulator can be as follws;

$$v_{ds\_error}^{e} = R_s(i_{ds}^{e} - i_{ds}^{e*}) - \omega_r L_s(i_{qs}^{e} - i_{qs}^{e*}) + \omega_r \lambda_f \sin\theta_{err} . \quad (7)$$

Considering that the currents are regulated by the current regulator without significient errors and the angle error, θ_{err}, is small.

The output voltage of the d-axis PI compensator can be expresed as follows;

$$\begin{aligned} V_{ds\_fb}^{e} &\approx v_{ds\_error}^{e} \\ &\approx \omega_r \lambda_f \sin\theta_{err} \\ &\approx \omega_r \lambda_f \theta_{err} \end{aligned} \quad (8)$$

In the proposed estimator of Fig. 4, the error signal of (8) is processed by the PI compensator to derive the speed of the rotor and the angle of the rotor is calculated by integrating the estimated speed. In a conventional method [3], the differentiation process is used to calculate the speed but this makes the system vulnerable to the noise. The experimantal study has shown that the proposed estimator provides very accurate and robust speed information for the application. But at the zero and low speed, the back-emf voltage is not high enough for the proposed vector control. Hence for the seamless operation from the zero speed, the current has been controlled with a contant magnitude and a pre-patterned frequency. And the angle for the synchronous reference frame is derived by integrating the frequency. In the experiment, the motor is started by the constant current control with pre-patterned frequency and at the speed of 12,000 r/min, the control is switched to the sensorless vector control. Fig. 5 shows the frequency pattern for the starting. As shown in step (I) of Fig. 5, the initial value of the frequency pattern is set to small constant speed, $\omega_{r\_start}^{*}$, for the initial alignment of rotor. After the alignment, the motor is accelerated according to the pattern of step (II). And then at step III, the motor is controlled by proposed sensorless control.

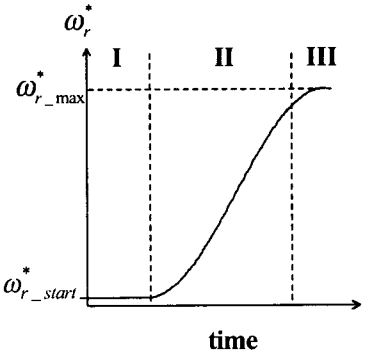

Fig. 5. Frequency pattern for constant current control.

V. Experimental Result With Sensorless Control

The experimenatal results with the proposed sensorless control are presented in Fig. 6 and Fig. 7. Fig. 6(a) shows the starting characteristics from zero speed to 20,000 r/min. The

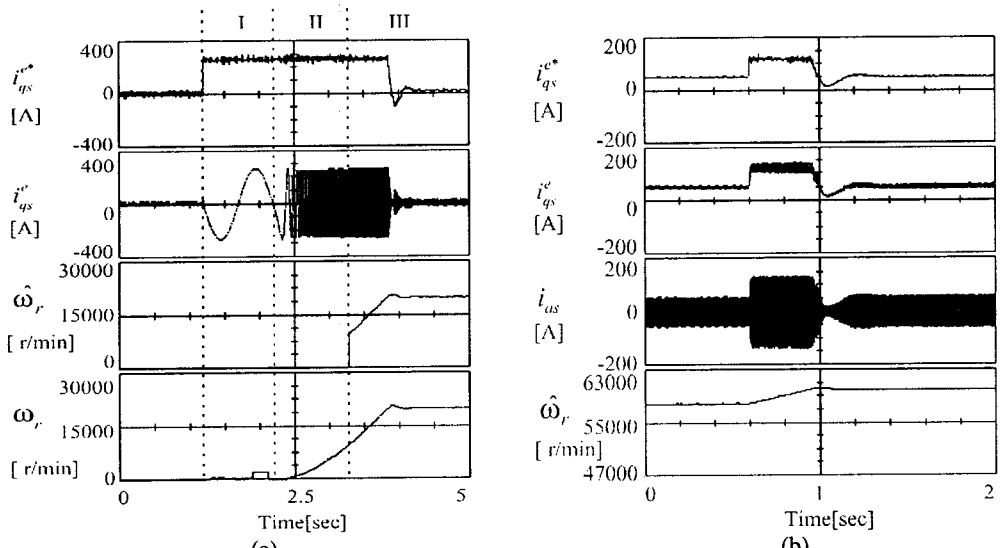

Fig. 6. Acceleration characteristics of the PMSM with the sensorless vector control scheme.
(a) Starting from zero speed. (b) Acceleration from 58,000[r/min] to 60,000[r/min].

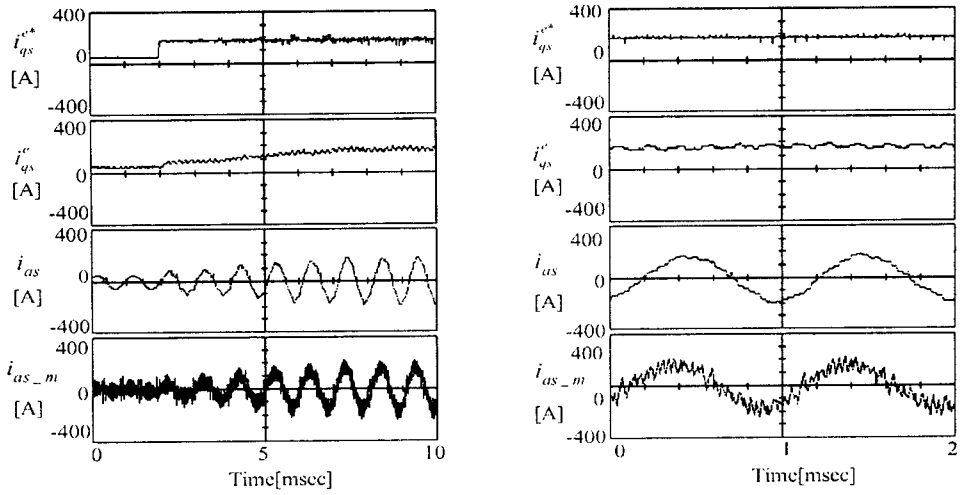

(a) (b)

Fig. 7. Current waveforms with proposed sensorless control (Acceleration from 58,000 r/min to 60,000 r/min).
(a) Current Waveforms. (b) Magnified figures of the last two periods of current waveforms in (a).

PMSM is accelerated by the rotating current vector with pre-calculated frequency pattern of Fig. 5. For the alingment of the rotor, the current vector is rotated with the starting frquency, $\omega^*_{r\_start}$, of 1 Hz as shown in step I. The proposed sensorless control of the step III is activated from 12,000 r/min and the speed is estimated. The bottom of Fig. 6(a) shows the measured speed using the hall-effect sensors. The test results in Fig. 6(a) show that the PMSM is effectively accelerated up to the thereshold speed by the proposed starting sequence and that the speed is clearly estimated by the proposed sensorless algorithm.

Fig. 7(b) shows the acceleration characteristics from 58,000 r/min to 60,000 r/min. The torque axis current is well controlled and the phase current is harnessed without overshoot by the synchronous current regulator. And the results show that the proposed control has enough speed control dynamics for the turbo-compressor.

Fig. 7 shows the performance of current regulator with the proposed sensorless control. For the experiment, the bandwidth of current regulator is set to 3,000 rad/sec. The current is measured at the acceleration from 58,000 r/min to 60,000 r/min. As shown in Fig. 7(a), in spite of the high excitation frequency of 1 kHz, the q-axis current, i^e_{qs}, tracks the command with small ripple current, which is caused by the dead-time and zero-current clamping effects. The bottom graph shows the the measured phase current, $i_{cs\text{-}m}$, which is measured by the current probe set (Tektronix AP504CX and AM503B). By the extremly small stator inductance, the fundmental current is accompanied by the significient ripple current, whch is caused by the 15 kHz PWM switching.

Fig. 7(b) shows the magnified waveforms of the last two periods of (a). The graphs show that the phase current is controlled sinusoidally by precisely sampling the fluctuating current.

VI. Conclusion

The development of the super-high speed drive for the 131kW 70,000 r/min PMSM for the turbo-compressor has been discussed. The synchronous reference frame current regulator has been implemented with the challenging requirements such as the low stator inductance(28μH) and the high dc link voltage(600V). And the experimental results of the current regulator operating up to 1,200 Hz are presented. To overcome the problem of the position sensor for the super-high speed operation, a new vector control scheme without position sensor has been proposed. At the scheme, a new position and speed estimator has been proposed. The proposed estimator can provide the reliable angle and speed information, which is robust to the measurement noise. The experimental results of the sensorless vector control scheme operating up to 60,000 r/min show the validity of the proposed control.

References

[1] Hamilton, S.L.," Micro turbine generator program," *Proceedings of the 33rd Annual Hawaii International Conference on System Sciences, 2000.*, Volume: Abstracts , 2000 , pp103 –103

[2] Soong, W.L.; Kliman, G.B.; Johnson, R.N.; White, R.A.; Miller, J.E. ,"Novel high-speed induction motor for a commercial centrifugal compressor ," *IEEE Trans. on Ind. Applicat.*,, Volume: 36 Issue: 3 , May/June 2000, pp 706 - 713

[3]Longya Xu; Changjiang Wang , "Implementation and experimental investigation of sensorless control schemes for PMSM in super-high variable speed operation ," in *Conf. Rec. IEEE-IAS Annu, Meeting*, 1998, vol.1, pp483 –489

[4] Mekhiche, M.; Kirtley, J.L.; Tolikas, M.; Ognibene, E.; Kiley, J.; Holmansky, E.; Nimblett, F, "High speed motor drive development for industrial applications,"in *Interna-*

tional Conference IEMD '99,1999, pp 244 -248
[5] T.R.Rowan and R.L. Kerkman, "A New Synchronous current Regulator and an analysis of current-regulated PWM Inverter ," *IEEE Trans. on Ind. Applicat.*, vol IA-22, pp678-690,July/Aug. 1986.
[6] D.W.Novotony and T.A.Lipo, *Vector Control and Dynamics of AC Drives*, Oxford University Press, New York, 1996
[7] Jong-Woo Choi, Seung-Ki sul, 'Inverter Output Voltage Synthesis Using Novel Dead Time compensation' *IEEE Trans, on Power. Appl.* Vol.11, No.2, March, 1996, pp.221-227
[8] Jong Woo Choi and Seung Ki Sul, 'New Dead Time compensation Eliminating Zero Current Clamping in voltage-Fed PEM Inverter', in *Conf. Rec. IEEE-IAS Annu, Meeting*, 1994, pp.977-984
[9] V. Blasko, V. Kaura and W. Niewiadomski, "Sampling of Discontinuous Voltage and Current Signals in Electrical Drives: A System Approach," *IEEE Trans. on IA*, Vol. 34, No. 5, pp 1123 -1130,1998.
[10] Seung-Ho Song, Seung-Ki Sul,Seung-Ho Song, Jong-Woo Choi, and Seung-Ki Sul, 'Digitally Controlled AC Drives', *IEEE Industry Applications Magazine*, July/August, 2000, pp.51-62
[11] T.Ohmae et al.,"A Microprocessor-Controlled High Accuracy Wide-range Speed Regulator for Motor Drives," *IEEE Trans. on IE*, vol IE-29,no.3, Aug. 1982, pp207~211